Source parameters for earthquakes in the northern North Sea

JENS HAVSKOV & HILMAR BUNGUM

Havskov, J. & Bungum, H.: Source parameters for earthquakes in the northern North Sea. *Norsk Geologisk Tidsskrift*, Vol. 67, pp. 51–58. Oslo 1987. ISSN 0029-196X.

A source parameter (focal mechanism) analysis has been conducted for six recent earthquakes in the northern North Sea: one magnitude (M_L) 4.3 event in the Viking Graben in 1982, one M_L 4.6 event at Stord in 1983, and four smaller (M_L 2.8–3.1) events further north in 1985. The Viking Graben earthquake shows oblique normal faulting consistent with NW-SE extensional tectonics, the Stord earthquake shows oblique thrust faulting consistent with E-W horizontal compression, while the smaller events further north (near 61.5°N, 4°E) are mostly of the strike-slip type with a NE-SW orientation of the compressional axis and a NW-SE orientation of the tensional axis. Within these parts of the North Sea and western Norway, the stress-generating situation is multifactional, with probably quite complicated interactions between long term tectonic causes of seismicity and more short term post-glacial rebound effects.

J. Havskov, Jordskjelvstasjonen, Universitetet i Bergen, N-5014 Bergen U., Norway.
H. Bungum, NTNF/NORSAR, Postboks 51, N-2007 Kjeller, Norway.

The large offshore investments in the North Sea recently have created a need for more reliable earthquake hazard estimations. This has in turn led to a complete reevaluation of the historical seismicity (Muir Wood et al. 1985) as well as of recent seismicity (Bungum et al. 1986b) in the area. It has also led to the establishment of new microseismic networks in western Norway (Engell-Sørensen & Havskov 1986) and in northern Norway (planned for 1987). From the seismicity maps in Fig. 1, it can be seen that the earthquakes in the northern North Sea and western Norway are generally confined to two areas, along the coast and in the Viking Graben. The two zones are separated south of about 61°N, while they merge into one broad zone further

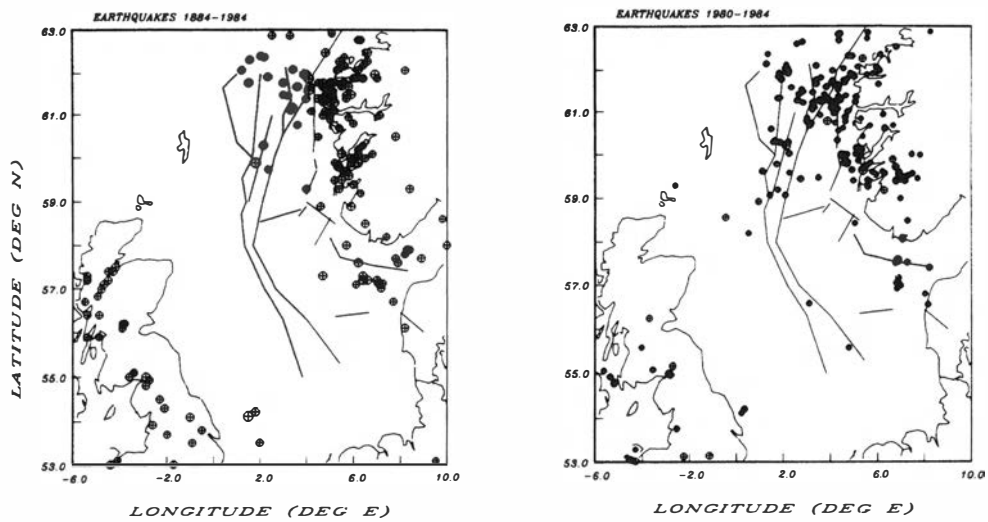

Fig. 1. Distribution of earthquakes in the northern North Sea and western Norway. The map to the *left* covers historical seismicity, 1834–1984 (from Muir Wood et al. 1985) while the one to the *right* covers contemporary seismicity, 1980-1984 (from Bungum et al. 1986b).

north. Analyses of the seismic hazard have shown that the two zones have about the same potential for larger earthquakes (Bungum et al. 1986a).

Seismotectonic interpretations of data on earthquake occurrence require, in addition to information concerning the temporal and spatial distributions, also knowledge about the faulting mechanisms and thereby about the stress patterns. Recently, there have been two earthquakes large enough to provide a good coverage of seismic recordings, in this paper we report on the solutions obtained. The two events occurred in the Viking Graben on July 29, 1982, and near Stord, western Norway, on March 8, 1983. The new seismic stations which came into operation in western Norway in 1984/85 have, moreover, now given us an opportunity to compute focal mechanism solutions for smaller earthquakes too; five such events from the northern North Sea are reported in this paper.

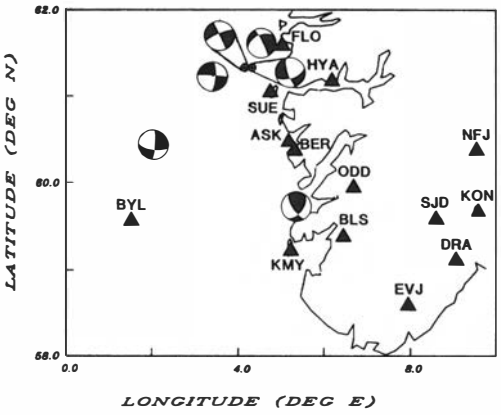

Fig. 2. Location of the earthquakes analyzed in this paper (with focal mechanisms) together with seismological stations (triangles) used in the analysis. The operation of the stations to the southeast (except KON) was discontinued in 1983, and those along the coast (except BER) started up in 1984/85.

The Stord earthquake, March 8, 1983

This earthquake, with a local magnitude (M_L) of 4.6, is the first event sufficiently large and sufficiently near the new stations in western Norway to permit a more precise determination of source parameters, as well as an analysis of aftershocks. It is seen from Fig. 2 that this event was more or less surrounded by stations. Within 250 km there were 9 stations, including one ocean bottom seismometer (BYL), and within 75 km there were three stations (ASK, BER and BLS). Digital data were available from six of these closer stations, and data (both digital and analog) were obtained from a large number of more distant stations throughout Europe, to be used in the estimation of the fault plane solution.

Main shock and aftershock hypocenters

Only stations within 250 km (Fig. 2) were used in determining the hypocenter, and precise S-readings were used for the two nearest (BLS and BER). Two crustal models for the area (Table 1) show Moho depths of 30 km with increasing depths inland (Sellevoll & Warrick 1971, Kanestrøm & Nedland 1975). Both models give a Moho velocity of 8.05 km/sec. We chose initially the simpler Model I given by Sellevoll & Warrick (1971).

The focal depth of the main shock was initially determined to 18 km based on the arrival times of some clear Moho reflections (1.25 secs after P on BER) seen on all aftershock recordings both for P and S waves (see Fig. 3). In addition, a clear arrival was observed 0.43 secs after P on the BER records and interpreted as a reflection from a layer between the hypocenter and Moho. This did fit Model II quite well (Kanestrøm & Nedland 1975). Keeping velocities fixed, the depths to the second interface and to Moho were varied by trial and error to fit the arrival times within 50 msec (relative to P) of the two reflections. This gave the final Model III (Table 1) and a hypocentral depth of 15 km. The epicenter was now relocated using this final model and the location program HYPO78 (Lee & Lahr 1978). The earthquake

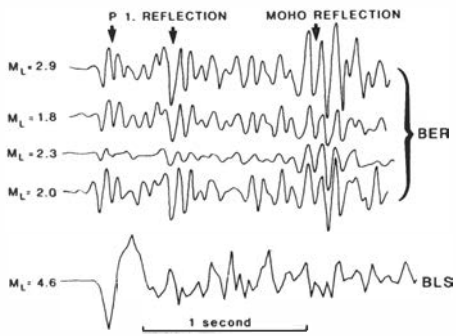

Fig. 3. P-waves of some aftershocks recorded in Bergen (top) and the main event recorded in BLS (bottom). Note that Moho and second layer reflections are not seen on BLS.

Table 1. Crustal models for western Norway. Depth to interfaces is in km and P-wave velocity in km/sec. Model I is from Sellevoll and Warrick (1971), Model II is from Kanestrøm and Nedland (1975) and Model III is from this paper. For the first model, a linear velocity gradient in the first layer has been approximated with a constant velocity.

Model 1		Model 2		Model 3	
Depth (km)	Velocity (km/s)	Depth (km)	Velocity (km/s)	Depth (km)	Velocity (km/s)
15	6.2	12	6.3	12	6.2
30	6.5	22	6.6	21	6.6
>30	8.05	30	7.1	31	7.1
		>30	8.05	>31	8.05

was located in this way at a depth of 13 km, indicating that the predicted arrival times from Model III for primary arrivals as well as secondary reflections fit the observed data quite well. The hypocentral depth of 15 km is considered to be accurate to within ± 2 km, and the Stord event is therefore the first major earthquake in western Norway to have a firmly established depth. The epicentral coordinates were 59.7°N and 5.4°E (Fig. 4 and Table 2).

Within two days, 19 aftershocks (M_L = 1.1–2.6) were recorded on the nearest stations. Observable differences in arrival times of direct and Moho reflected phases varied less than 25 msec between events corresponding to depth variation of less than 250 m. Using one aftershock as a master event, the four largest aftershocks were located using stations BER, SJD, EVJ and DRA (Fig. 2). Depth was fixed at 15 km, and the epicenters (Fig. 5) indicate a NW-SE lineation. The main shock could not be accurately located relative to the reference event since the BER recordings were saturated. However, variation in relative arrival times between the main event and aftershocks for SJD, EVJ and DRA were less than 50 msec, indicating that the aftershocks were very close to the main event.

Fault plane solutions

A fault plane solution for the 1983 Stord earthquake has been obtained using 23 stations at distances up to 1600 km (Fig. 6). For stations SJD, EVJ, DRA and NFJ both direct and refracted arrivals were used; thus they are plotted twice. A fortunate coincidence was the change of polarity of first arrivals within the NORSAR array, which in this case has been crucial in restricting one of the fault planes. The fault plane solution shows an oblique thrust fault with a certain horizontal component, and with the compressional axis going east-west. More details on the solution are

Table 2. Source parameters for the six earthquakes analyzed in this paper. No. 1 is the 83/03/08 Stord earthquake, no. 2 is the 82/07/29 Viking Graben earthquake, and 3–6 are five smaller earthquakes from the northern North Sea. The first 8 lines are date, origin time, epicenter latitude and longitude (degrees), focal depth (km), M_L magnitude, log seismic moment (dyne-cm), and source radius (m). Then follow strike, dip and slip (degrees) for each of the two nodal planes, P- and T-axis orientations (strike and plunge), greatest horizontal compression and tension (azimuth and size for each), relative size of the horizontal deviatoric stress field, and the sum of the squared difference between observed and theoretical S_v/P amplitude ratio.

Event No:	1	2	3	4	5	6
Yr/Mo/Day	83/03/08	82/07/29	85/09/08	85/10/01	85/10/27	85/11/30
Origin time	18.43.58	00.17.06	12.31.58	13.31.10	04.36.21	19.05.13
Lat. (deg.)	59.7	60.4	61.3	61.3	61.3	61.6
Lon. (deg.)	5.4	2.0	3.4	4.2	4.3	4.6
Depth (km)	15	17	19	15	15	6
Magnitude ML	4.6	4.3	3.1	3.0	2.8	3.0
Log Moment	21.3					
Radius (m)	250–500					
Strike angles	35:145	100:186	273:184	334:64	67:345	337:62
Dip angles	52:67	63:99	86:106	90:102	59:103	85:138
Slip angles	−150:−42	170:−27	15:−176	168:0	15:−148	132:−7
P-axis	267:9	320:25	227:14	200:9	30:32	212:36
T-axis	6:46	55:12	319:8	109:8	293:12	99:28
P-hor. azimuth	270	323	228	199	26	200
P-hor. size	−0.97	−0.81	−0.94	−0.98	−0.72	−0.60
T-hor. azimuth	180	53	318	109	296	110
T-hor. size	0.48	0.95	0.98	0.98	0.95	0.73
Hor. dev. stress	0.72	0.88	0.96	0.98	0.84	0.66
Error	—	—	0.073	0.059	0.088	0.013

given in Table 2 (Event 1), and it is seen there that the direction of the slip is near 45°. Also given there are the directions and sizes of the greatest horizontal compression and tension, as well as the relative size of the horizontal deviatoric stress field (Slunga 1981). The last parameter describes the horizontal significance of the stress, or the 'fraction' of the principal stresses that are confined within the horizontal plane. Defined in this way, the size of the horizontal deviatoric stress field is 1.0 for a vertical-dip stike-slip event, and 0.0 for a vertical-slip dip-slip event (for more details, see Kibsgaard 1985).

A fault plane solution obtained in this way is ambiguous with respect to choosing one of the nodal planes as the fault plane. Additional information needed for resolving this is in the present case, provided by the geological structures in the area (Fig. 4) as well as by the lineation of aftershocks (Fig. 5), all pointing towards the NW-SE oriented plane as the plane of rupture. Within this interpretation, it is inferred that the horizontal part of the motion is right-lateral, as indicated in Fig. 5.

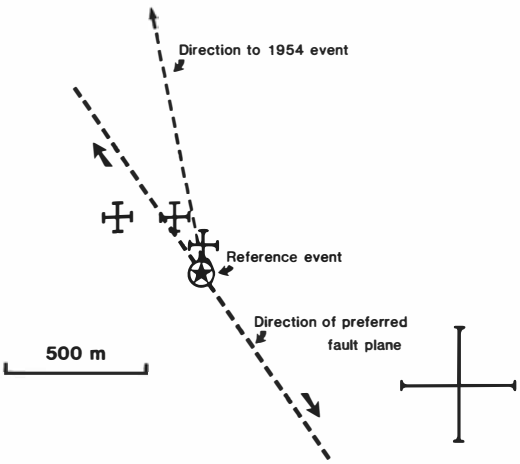

Fig. 5. Locations of aftershocks following the 1983 Stord earthquake. The locations of four aftershocks are indicated, with bars reflecting location uncertainties. The direction of the preferred fault plane is also given, as well as the direction to the 1954 events (about 10 km away).

The 1954 Stord earthquakes

Two relatively large earthquakes in the area occurred in 1954 on July 7, when two events of magnitudes around 5 occurred within 23 minutes. These earthquakes were originally located to about 25 km west of the 1983 event (Sellevoll 1982). A reexamination of the original data, however, showed almost identical arrival times (relative to BER) for the two events using the nearest stations Bergen, Copenhagen and Uppsala. This permitted the arrival times relative to BER to be averaged, and the average location of the two events was then calculated relative to the 1983 event (Fig. 4). Sellevoll (1957) found, by analyzing the arrival times of Pg, Pn and sP, that the depth was about 16 km, which agrees quite well with our depth estimate for the 1983 Stord event. Thus the depth was restricted to 15 km and the epicenter of the 1954 events was estimated at 59.8°N and 5.3°E, or about 10 km NNW of the 1983 event. With the uncertainty of these relocations it is therefore quite possible that the 1954/7/7 and the 1983/3/8 earthquakes occurred on the same fault (see Figs. 4–5).

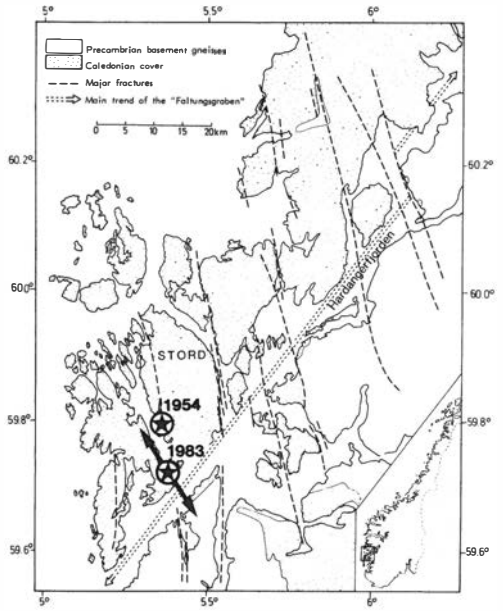

Fig. 4. Geology of the Stord area (from Færseth et al. 1976). The epicenters of the 1954 and 1983 events are shown with encircled stars and the arrows on the latter indicate likely surface projection of the fault plane.

Other source parameters

The nearest station giving unsaturated digital signals of the main 1983 Stord event was BLS (Fig. 2). These data were used for computation of source-displacement spectra, based on the following relationship:

$$M_\omega = 4\pi\rho D\beta^3 P_s^{-1} R_s^{-1} \Omega_\omega$$

where ω is angular frequency, ρ is density, D is hypocentral distance, β is shear wave velocity, P_s is a path correction term, R_s is the radiation pattern coefficient, and Ω_ω is the (S-wave) displacement spectrum. The seismic moment M_o is the low-frequency value of the source-displacement spectrum. The results of this analysis on the BLS data give a seismic moment M_o of around 2×10^{21} dyne-cm, and with an M_L value of 4.6 this gives a reasonable M_o/M_L relationship (Bungum et al. 1982).

The source-displacement spectrum also normally provides possibilities for computation of source radius, stress drop and displacement across the fault. This, however, requires the corner frequency to be known, and it has not been possible in this case to estimate this sufficiently accurately from the source displacement spectrum. Another method has therefore been chosen, based on the time difference T between the P-wave onset and the first zero crossing. Frankel & Kanamori (1983) demonstrated that the duration of the rupture could be obtained simply from the difference ΔT between T from the main shock and T from an aftershock, thus making it very simple to obtain rupture duration without knowing details of the medium. Data from the two nearest stations (BLS and SJD) with unsaturated recordings gave ΔT values of 50 and 37 msec, respectively.

This approach also makes it possible to compute source radius. Assuming a circular fault with radius r and constant rupture velocity v, we have

$$r = \frac{\Delta T \cdot v}{1 - \frac{v}{c}\sin\theta}$$

as given by Boatwright (1980). Here c is the P-wave velocity and θ is the angle between the normal to the fault plane and the outgoing seismic ray. The velocity v = 6.6 km/sec and c is assumed 0.9 times the shear wave velocity. The angle θ was measured for the two possible rupture planes, where the one striking NE-SW gave 150 m for BLS and 240 m for SJD, while the one striking NW-SE gave 250 and 270 m, respectively. The best agreement with observations is thus obtained for the NW-SE striking plane, which is the one preferred also for other reasons, as discussed above.

Having an estimate for source radius r and seismic moment M_o, we can then calculate stress drop $\Delta\sigma$ and displacement μ across the fault using the circular source model of Brune (1970, 1971):

$$\Delta\sigma = \frac{7}{16} \cdot \frac{M_o}{r^3}\,;\; u = \frac{1}{\pi\mu} \cdot \frac{M_o}{r^2}$$

The values obtained for these parameters, with the rigidity modulus μ set to 3.3×10^{11} dyne/cm^2, are very sensitive to source radius as shown in Table 3. The values there indicate that a source radius of less than 250 m gives unrealistically high values both for stress drop and displacement, and also that a radius of 1000 m probably is the upper limit.

The Viking Graben earthquake, July 29, 1982

It is seen from Fig. 1 that there is a relatively high seismic activity in the Viking Graben area, where one of the larger earthquakes in the last few years occurred on July 29, 1982. The magnitude for this earthquake was 4.3 M_L as compared to 4.6 for the Stord earthquake, and the location, based on 81 readings, was near 60.4°N, 2.0°E. This is near the western flank of the Viking Graben, as seen from Fig. 1. Given the area, it is difficult to obtain a reliable estimate of focal depth, but we have found, for a variety of crustal models, that a depth of 15–20 km satisfies the observations better than shallower depths.

A fault plane solution for the 1982 Viking Graben earthquake is shown in Fig. 6, with parameters given in Table 2 (Event 2). This solution is more uncertain than the one for the 1983 Stord earthquake, with some discordant points, but there is not much doubt about the general interpretation in terms of normal faulting. The amount of obliqueness in the solution is dependent upon the detailed interpretation, but the tensional axis will in any case be oriented NE-SW, and the compressional axis NW-SE. From the seismological data alone it is not possible in this case

Table 3. Relations between source radius, stress drop and displacement across the fault for the 1983 Stord earthquake.

Source radius (m)	Stress Drop (bars)	Displacement (cm)
125	450	124
250	56	31
500	7	8
1000	0.9	1.9

to resolve the fault plane ambiguity, but based on the geological information from the area it is natural to suggest that the NS-oriented nodal plane is the one along which the faulting has taken place. That plane dips about 80° to the east, and the strike-slip component caused by the obliqueness will in that case have a left-lateral sense of motion.

Solutions from S_v/P amplitude ratios

By 1985, a number of new seismic stations along the coast of western Norway were in operation (see Fig. 2), and this provided new possibilities for better detectability and more precise earthquake locations (Engell-Sørensen & Havskov 1985), as well as for new focal mechanism solutions. However, the method of P-wave first motions cannot be used in this case (for smaller earthquakes), because of too low signal-to-noise ratios and too few stations. To obtain fault plane solutions in this case, methods involving some sort of theoretical amplitude modelling must be used. One of the simplest methods available here is the one based on comparison between theoretical (computed) and observed S_v/P amplitude ratios (Kisslinger 1980), a method which has been successfully applied to earthquakes in the Oslo Graben area (Kibsgaard 1985).

The S_v/P amplitude ratio method has been applied to four earthquakes occurring north of the two already analyzed. The events are Nos. 3-6 in Table 2, where it is seen that they occurred between September 8 and November 30, 1985, with magnitudes (M_L) from 2.8 to 3.1. The method is essentially based on the fact that the amplitudes of the body waves (P and S) observed at a particular azimuth and distance are determined by the focal mechanism. The use of amplitude ratios simplifies the approach because problems of instrument calibration can then be neglected, and because transmission coefficients across internal boundaries can also be neglected since their ratio does not differ much from one. The free surface factor, however, must be accounted for in the computations.

The S_v/P method is applied iteratively by looping through a large number of combinations of strike, dip, and slip values in the search for a minimum in the sum of the squared difference between the observed and the theoretically calculated amplitude ratio (see Table 2). If nothing is known about the solution in advance, this involves a considerable computational load, but this can normally be reduced by using first motion polarity data in constraining the starting solution. In the present case this was difficult because of the problems in reading first motions, and there were also some problems because of large epicentral distances. First motion data have, however, been used in constraining the solutions in cases with basic ambiguities.

The results obtained are given in Table 2, the solutions are plotted in Fig. 2, and in Fig. 7 we plot the locations of the P and T axes as well as the directions and the sizes of the greatest horizontal compressions (solid lines) and tensions (dotted lines). It is seen that the solutions are predominantly strike-slip with a large horizontal significance (with the exception of event 6 where there is a component of normal faulting), and although the orientations of the nodal planes vary

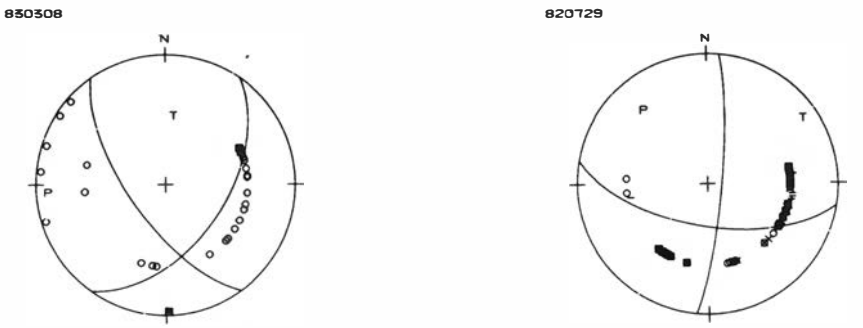

Fig. 6. Fault plane solutions for the 1983 Stord (left) and the 1982 Viking Graben (right) earthquake in an equal-area lower hemisphere projection. The solutions are based exclusively on first-motion polarity for P waves, with open circles for dilatations and filled squares for compressions. P and T indicate the axes of maximum and minimum compressive stress, respectively. More details for the solutions are given in Table 2.

a great deal it is interesting to note that the orientations of the stress axes are quite consistent for the four events: the compressional axes are all oriented NE-SW and the tensional axes NW-SE (Fig. 7). This is different from both the Stord and the Viking Graben earthquakes, indicating that the area further north is subjected to a different tectonic regime.

Discussion

The 1983 Stord event seems to be a classical case of a mainshock-aftershock sequence. The lineation of the aftershocks and the source radius calculations indicate that the NW-SE striking nodal plane represents the fault plane. The 1954 events did occur very close to the 1983 event. However, the hypocenter precisions of the 1954 events are too low to say definitely if the events occurred on the same fault. In any case it is clear that major earthquake activity reoccurs within the same limited area. Fig. 3 shows the main geological features of the region, the epicenters of the 1954 and 1983 events and the likely surface orientation of the 1983 faulting. It seems that the Stord event is correlated with the nearly NS striking fractures and not the more dominating NE-SW striking Caledonian faults.

The seismotectonics of this area has been discussed in a number of recent papers (Muir Wood 1985, Muir Wood et al. 1985, Bungum et al. 1986a, b). It is noteworthy in the present context that while the Stord earthquake shows thrust faulting, the Viking Graben earthquake shows normal faulting, with inferred axis of maximum stress E-W compressional in the first case and NE-SW tensional in the latter case. For the seismically active area (see Fig. 1) between the northeastern corner of the North Sea and the southeastern corner of the Møre Basin (61.2–61.7°N, 3.4–4.6°E), four new focal mechanism solutions (albeit more poorly constrained) show a predominance for strike-slip faulting, with the axes of maximum horizontal tension oriented NW-SE. According to Hamar & Hjelle (1984), this area is dominated by NNW-SSE oriented normal faults, and they also note that strike-slip lateral faulting seems to be quite common in this area as well as over most other parts of the Norwegian Continental Shelf. This is consistent with Muir Wood (1985), who notes that the regional tectonics in the North Sea (outside the post-glacial rebound domes of Scotland and Fennoscandia) appears to be chiefly extensional with strike-slip faulting.

Conclusions

We conclude this paper by pointing out the following:

(1) The Viking Graben earthquake mechanism is consistent with the assumption that this area is still subjected to extensional movements.

(2) The Stord earthquake mechanism reveals a compressional stress orientation which is consistent with what is observed in other parts of Scandinavia (Kibsgaard 1985, Slunga 1985) as well as in most of northwestern Europe (Ahorner 1975, Bonjer et al. 1984). It is reasonable to assume that this reflects stress-generating mechanisms of plate-related origin (Bungum & Fyen 1980).

(3) It is also likely that the earthquake activity along the coast of western Norway is related to post-glacial uplift, which would give stress patterns of the same type (Muir Wood 1985). Even though the largest movements take place immediately following the deglaciation

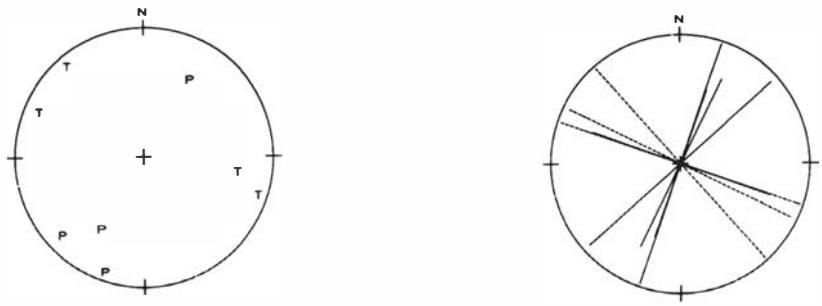

Fig. 7. For events 3–6 in Table 2, this Fig. shows the locations of the axes of maximum compression P and tension T (left), together with the directions and the sizes of the greatest horizontal compressions (solid lines) and tensions (dotted lines).

(Muir Wood & Lagerbäck 1985), the uplift is still significant.

(4) The seismically active area outside northwestern Norway (near 61.5°N, 4.0°E) seems also to be subjected to extensional tectonics (NW-SE), with a preference for strike-slip faulting. This is consistent with North Sea conditions at large.

The interaction between the long term tectonic causes of seismicity and the short term post-glacial rebound effects is probably quite complicated, and requires to be addressed both theoretically (through modelling) and observationally. The basis for such work is now rapidly being improved because of new microearthquake networks both in Western Norway (in operation by 1985) and in Northern Norway (planned for operation by 1987).

Acknowledgements. – This research, NORSAR contribution No. 368, was completed under the project 'Earthquake Loading on the Norwegian Continental Shelf' supported by the Royal Norwegian Council for Scientific and Industrial Research (NTNF), Statoil a.s., Norsk Hydro a.s., A/S Norske Shell, and Esso Norge a.s.

Manuscript received May 1986

References

Ahorner, L. 1975: Present-day stress field and seismotectonic block movements along major fault zones in Central Europe. *Tectonophysics 29,* 233–249.

Boatwright, J. 1980: A spectral theory for circular seismic sources: simple estimates of source dimension, dynamic stress drop and radiated seismic energy. *Bull. Seism. Soc. Am. 70,* 1–28.

Bonjer, K.-P., Gelbke, C., Gilg, B., Rouland, D., Mayer-Rosa, D. & Massinon, B. 1984: Seismicity and dynamics of the Upper Rhinegraben. *J. of Geophys. 55,* 1–12.

Brune, J. N. 1970: Tectonic stress and the spectra of seismic shear waves from earthquakes. *J. Geophys. Res. 75,* 4997–5009.

Brune, J. N. 1971: Correction. *J. Geophys. Res. 76,* 5002.

Bungum, H. & Fyen, J. 1980: Hypocentral distribution, focal mechanisms, and tectonic implications of Fennoscandian earthquakes, 1954–1978. *Geol. Fören. Stockholm Förhl. 101,* 261–273.

Bungum, H., Havskov, J., Hokland, B. K. & Newmark, R. 1986a: Contemporary seismicity of northwest Europe. *Annales Geophysicae, 4B,* 567–576.

Bungum, H., Vaage, S. & Husebye, E. S. 1982: The Meløy earthquake sequence, northern Norway: source parameters and their scaling relations. *Bull. Seism. Soc. Am. 72,* 197–206.

Bungum, H., Woo, G. & Swearingen, P. H. 1986b: Earthquake hazard assessment in the North Sea. *Phys. Earth & Planet. Inter. 44,* 201–210.

Engell-Sörensen, L. & Havskov, J. 1985: Recent North Sea seismicity studies. Paper given at IASPEI General Assembly in Tokyo, August 19–30, 1985.

Frankel, A. & Kanamori, H. 1983: Determination of rupture duration and stress drop for earthquakes in Southern California. *Bull. Seism. Soc. Am. 73,* 1527–1551.

Færseth, R. B., Macintyre, R. M. & Naterstad, J. 1976: Mesozoic alkaline dykes in the Sunnhordland region, western Norway; ages, geochemistry and regional significance. *Lithos 9,* 331–345.

Hamar, G. P. & Hjelle, K. 1984: Tectonic framework of the Møre Basin and the northern North Sea. *In: Petroleum Geology of the North European Margin,* Norwegian Petroleum Society (Graham & Trotman), 349–358.

Husebye, E. S., Bungum, H., Fyen, J. & Gjøystdal, H. 1978: Earthquake activity in Fennoscandia between 1497 and 1975 and intraplate tectonics. *Nor. Geol. Tidsskr. 58,* 51–68.

Kanestrøm, R. & Nedland, S. 1975: Crustal structure of southern Norway. A reinterpretation of the 1965 seismic experiment. Institute report, *Seismological Observatory, University of Bergen, 40 pp.*

Kibsgaard, A. 1985: *Focal mechanism studies of/by the SV to P amplitude ratio.* Thesis, University of Oslo.

Kisslinger, C. 1980: Evaluation of S to P amplitude ratios for determining focal mechanisms from regional network observations. *Bull. Seism. Soc. Am. 70,* 999–1014.

Lee, W. H. & Lahr, J. C. 1978: A computer program for determination of hypocenter, magnitude and first motion patterns of local earthquakes. *USGS* Open File Report 75–311.

Muir Wood, R. 1985: The seismotectonics of North-West Europe. *Proceedings, Conference on Earthquakes and Earthquake Engineering in Britain, University of East Anglia, 18–19 April 1985,* Thomas Telford Ltd., London, pp. 67–80.

Muir Wood, R. & Lagerbäck, 1984: Postglacial faulting and earthquakes in northern Scandinavia. Manuscript.

Muir Wood, R., Woo, G. & Bungum, H. 1985: The history of earthquakes in the northern North Sea. *In:* W. H. K. Lee, H. Meyers and K. Shimazaki (eds.), *Preliminary Proceedings from the IASPEI Symposium on Historical Seismograms and Earthquakes, Tokyo, Auust 27–28, 1985,* pp. 463–472.

Newmark, R. & Turbitt, T. 1985: Catalogue of North Sea earthquakes 1980 to 1984 and brief project summary. Report No. 246, *Global Seismology Unit, British Geological Survey,* Edinburgh, U.K., 25 pp.

Sellevoll, M. A. 1957: Earthquakes in the Norwegian Channel on the 7th and 10th of July 1954. *Universitetet i Bergen,* Årbok, Mat. Nat. ser. 2, 1–28.

Sellevoll, M. A. & Warrick, R. W. 1971: A refraction study of the crustal structure in southern Norway. *Bull. Seism. Soc. Am. 61,* 457–471.

Sellevoll, M. A., Almaas, J. & Kijko, A. 1982: A catalogue of earthquakes felt in Norway 1953–1975 and a statistical analysis related to the completeness of catalogues for earthquakes felt in Norway 1899-1979. Institute Report, *Seismological Observatory, University of Bergen.*

Slunga, R. 1981: Focal mechanisms of earthquakes in Scandinavia. A review. FOA 202, Stockholm.

Slunga, R., Norrman, P. & Glans, A.-C. 1984: Baltic Shield seismicity, the results of a regional network. *Geophys. Res. Lett. 11,* 1247–1250.